PROJECT REPORT

Experiment Ref. No. SC 2774
Title: “pH-driven transitions in 'smart' nanoparticles at the mesoscopic scale”

Beamline: BM02

Dates: 23 – 27 September 2009

Team

Dr. Francisco M. Goycoolea (USC, Spain)
Dr. Cyrille Rochas (CNRS, France)
Dr. David Laurent (U.Lyon)
Gustavo Rivera (USC, Spain)
Jorge Pinto (USC, Spain)
Davide Filotto (USC, Spain)
Ce Gynto (CNRS, France)

Abstract

As a part of a project focused on the design of novel biopolymer-based nanoparticle systems with bioresponsive properties for advanced drug delivery application, synchrotron SAXS studies allowed to study details of the structure of various nanoparticles comprsing chitosan and other polyelectrolytes at varying pH. In parallel, oil-core nanocapsule systems coated with chitosan of varying molecular weight and degree of acetylation have also been studied.

Introduction

Multi-functional nanodelivery systems that combine tissue– or organ–specific targeting, with therapeutic action are currently at the focus of innovations in drug delivery [1,2]. This type of vehicles is regarded as ‘smart’, ‘intelligent’ or ‘responsive’ drug delivery systems. Commendable progress in this direction has been achieved, particularly in the development of systems based on hydrogel materials able to respond by changing their volume, shape, permeability and mechanical strength in pronounced and predictable manner to a variation in either external physical factors such as temperature, pressure, light, or electrical stimuli, or chemical ones such as pH, solvent composition, ionic strength or specific substances [3]. However, far less research has been centered in nanoparticle systems able to respond to changes in their microenvironment. Polysaccharide-based nanoparticles can be made under aqueous and fairly mild conditions, thus effectively, being especially suitable to preserve the bioactive conformation of delicate macromolecules (e.g. hormones, antigens, DNA, siRNA, growth factors), that otherwise would be prone to enzymatic degradation and hydrolysis. Also, hybrid core-shell nanoparticles comprising a synthetic polymer coated with a polysaccharide (e.g. dextran or heparin),

alternative to the use of polyethylene glycol, have been utilized as a successful 'stealth' strategy to increase the blood circulation time and to reduce the recognition of the nanoparticles by the mononuclear phagocyte system [4]. By contrast with 'hard–type' inorganic nanostructures (e.g. metallic nanoparticles, carbon nanotubes, etc), hydrogel nanoparticles made out of water–soluble polymers, can be regarded as 'soft' nanoscopic materials. This type of systems represents a special class of materials that is gearing the development of an increasing number of innovative applications, particularly in the biomedical field, as they are bound to exhibit far less toxicity than their inorganic counterparts.

Experimental

Instrument settings at BM02.

Beamline: BM02
E = 14 kEv (λ =0.897 Å)
Sample-to-detector distance: 1.51 m

The collected scattering data were calibrated on the basis of the known positions of silver behenate powder Bragg reflections.

The following experiments were conducted:

Experiment I. Nanoparticles of chitosan (CS) formed by ionotropic gelation with pentasodium triplyphosphate (TPP) without and with added polyanions of the following type:

1. CS-TPP [conc. 53 mg/mL]
2. CS-TPP-alginate (ALG) 6009 (Mw ~ 32000) [conc. 8.9 mg/mL]
3. CS-TPP-alginate (ALG) 7006 Mw ~ 7000) [conc. 27 mg/mL]
4. CS-hyaluronic acid (HA) (Mw ~ 39000) [conc. 52 mg/mL]

These nanoparticle systems were considered as "primary particles" in further experiments.

Experiment II. Primary nanoparticles of the same type as in Experiment I were crosslinked with genipin (GNP). The particles were previously crosslinked at the following GNP/NP mass ratios: 0.1, 0.2, 0.3 and 0.5 until equilibrium was reached [conc. 1 mg/mL].

Experiment III. The kinetics of surface crosslinking with genipin (GNP) of primary nanoparticles of the same type as in Experiment I [conc. 3 mg/mL] was studied.

Experiment IV. The particles of Experiment I and II were studied at varying pH in the appropriate buffer systems, namely:

a) Gastric buffer pH 1.2
b) Acetate buffer pH 4.5
c) Phosphate buffer saline pH 7.4
d) TRIS buffer pH 8.0

Experiment V. Nanocapsules prepared by spontaneous emulsification. We investigated the role of the degree of N–acetylation (DA) of chitosan (CS) of low and high M_w (~10 and ~110 kDa denoted here as LDP CS and HDP CS, respectively) on the structure of the obtained nanocapsules.

Results and discussion

Experiment I.

Figure 1 shows Porod plots in the form of $I(q)q^4$ *vs.* q for chitosan-based nanoparticles that were further utilized in subsequent surface crosslinking experiments. This included CS-TPP and CS-TPP added with alginate or hyaluronan. It was verified that all the systems exhibited $q^{\sim -4}$ dependence for $I(q)$ in the low q region (q<0.04 A^{-1}). The Porod law is well known to be valid for two-phase systems with a sharp boundary [5] and it also sensitive to several properties, such as shape, size, and to curvatures and roughness of the water/nanoparticle interface [6]. It is possible to appreciate that the shape of the curve for CS-TPP is substantially different to the rest at low and high q's. This indicates subtle differences in morphology at the local scale (e.g. in shell thickness). Also, it can be appreciated that the curves for nanoparticles that contain the two alginates of distinct molecular weight reveal qualitatively different plots, thus indicating possible differences in local organization

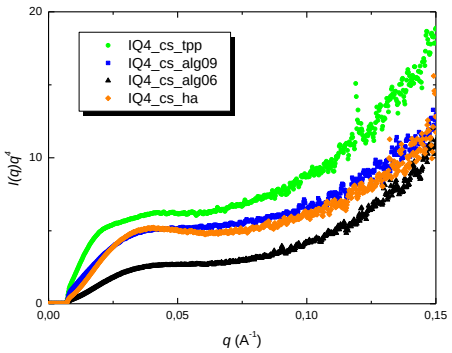

Figure 1. Porod plots ($I(q)q^4$ vs. q) recorded from SAXS measurements for chitosan-based nanoparticles in water (as indicated in labels).

associated with the size of the polyanion chains. While the curves for systems comprising HA seem very similar than that comprising alginate 7006 both at low and at high *q*'s. The observed differences point to the role of the polyanion in the local organization of the nanoparticles structure at the mesoscale and molecular level, in agreement with previous studies [7].

Experiment II.

The various types of "primary" chemically uncrosslinked nanoparticles described above were subjected to surface covalent crosslinking with genipin at varying GNP/NP mass ratios: 0.1, 0.2, 0.3 and 0.5 at total nanoparticle concentration of 1 mg/mL. Figure 2 shows the Porod plots obtained for the four types of addressed nanoparticle systems. Clearly, uncrosslinked nanoparticles (green traces) showed distintively different curves at low and high q's. Whereas crosslinking invariably led to large changes in the overall shape of the Porod curves. This can be considered as evidence that genipin crosslinking affects the interface between the nanoparticle and the solvent medium (water) and also suggest that there can be differences in the surface roughnes of each system. Besides, it is clear that the nature of the polyanion influences directly the observed patterns.

Experiment III.

The kinetics of surface genipin-crosslinking for the various types of nanoparticles was investigated. To this end, a core-shell model (Figure 3) was tested for fitness to the intensity scattering curves. SAXS scattering curves for the various systems were plotted in the form $I(q)q2$ *vs* $1/q^2$ and fitted in the linear region, as shown in Figure 4 for CS-TPP nanoparticles at varying degree of genipin crosslinking. Clearly, a high linear regression coefficient with a negative intercept B value were diagnostic that a core-shell structure was present. Figure 5 shows the estimated values of shell-thickness at varying genipin/nanoparticles mass ratios. Notice that the addition of genipin leads to a gradual increase in shell thickness (in the range 22.2 - 26.7 nm). By virtue of this analysis it was also possible to calculate the evolution of the thickness of nanoparticles' shell during the time course of the covalent reaction function at two varying degrees of genipin crosslinking (Figure 6). Notice that the SAXS scattering curves are essentially similar. The outcome of this analysis is shown in Figure 7 where it can be appreciated that genipin crosslinking leads to a monotonic moderate increase in the thickness of the pre-formed nanoparticles. The overall increment in shell thickness observed at equilibrium (<1.2 nm) accounts for ca. 10% of the original thickness. The corresponding Porod curves for the evolution of genipin crosslinking of CS-TPP are shown in Figure 8. In the series of curves it can be noticed that the intensity of the first maxima peak

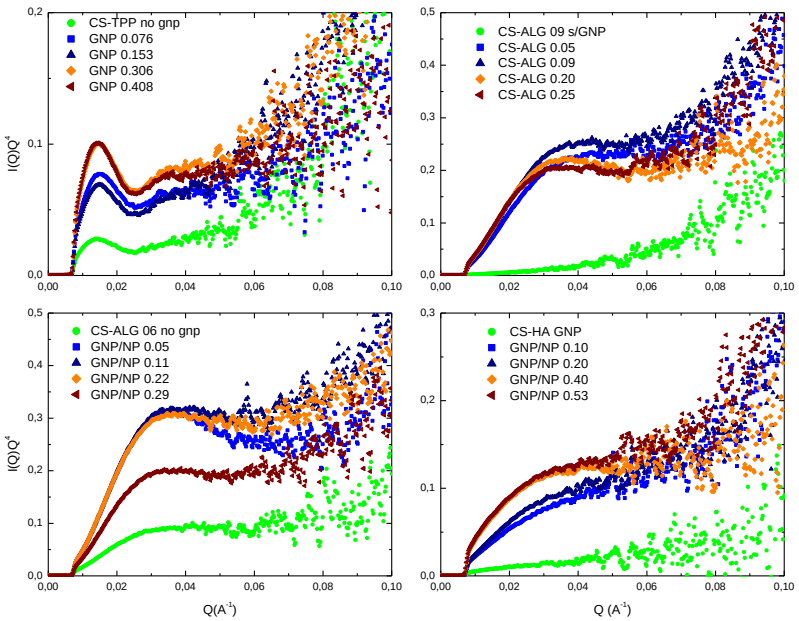

Figure 2. Porod plots ($I(Q)Q^4$ vs. Q) recorded from SAXS measurements for chitosan-based nanoparticles at varying degrees of crosslinking with genipin in water (as indicated in labels).

decreases as the crosslinking process takes place, concomitant to this, the minima through and second maxima peaks are displaced to gradually lower *q* values. These differences can be attributed to subtle variations in surface roughness of the nanoparticles. Altogether, the SAXS results on CS-TPP nanoparticles can be considered as diagnostic evidence that genipin crosslinking occurs preferentially at the nanoparticle's surface, in agreement with the original hypothesis of this study.

The same analysis was conducted on nanoparticles that contained alginates of both molecular weights, namely ALG 6009 and ALG 7006 and it was found that the shell thickness (Figure 9) was nearly an order of magnitude smaller and the effect of genipin reached its maximum after 25 h. In nanoparticles that comprised ALG 6009 it was not possible to fit the core-shell model, whereas in those comprising hyaluronic acid, shell thickness values of ~12.1 nm were measured. Transmission electron microscopy studies have revealed that a core shell structure does exist in CS-TPP based nanoparticles (results not shown).

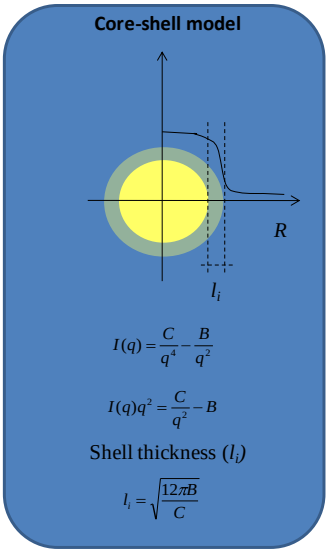

Figure 3. Core-shell model to estimate the particle shell thickness

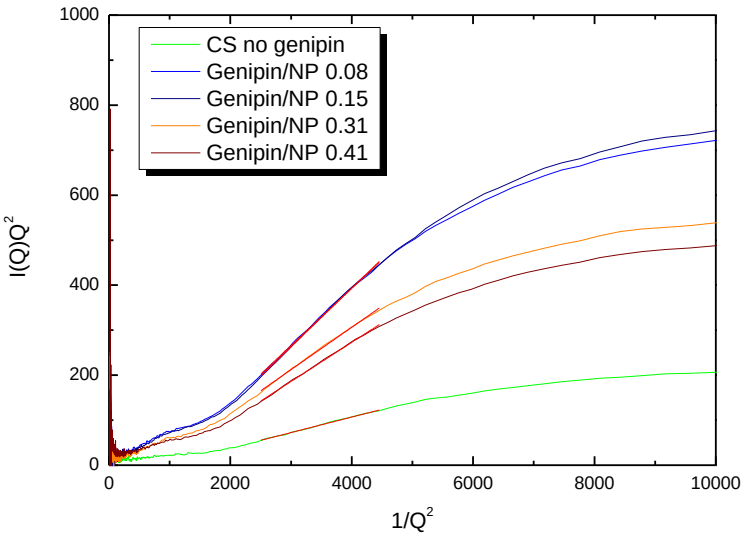

Figure 4. Core-shell model plots ($I(Q)Q^2$ vs. $1/Q^2$) applied to SAXS scattering curves for chitosan-TPP nanoparticles at varying degrees of crosslinking with genipin in water (as indicated in label).

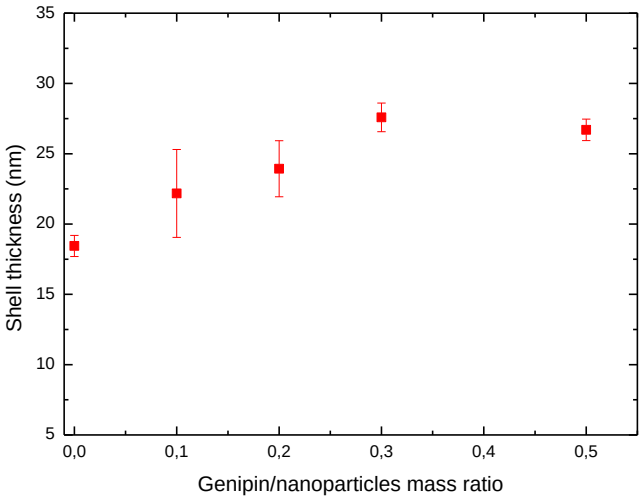

Figure 5. Shell thickness of CS-TPP nanoparticles crosslinked with genipin to varying extents at 37°C at pH 1.2.

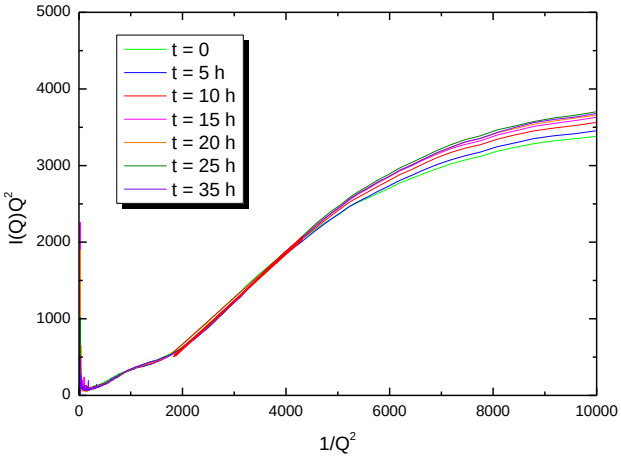

Figure 6 . Core-shell model ($I(Q)Q^2$ vs. $1/Q^2$) applied to SAXS scattering curves during time course crosslinking of chitosan-TPP nanoparticles with genipin (genipin/np mass ratio ~ 0.5) in water at 37°C.

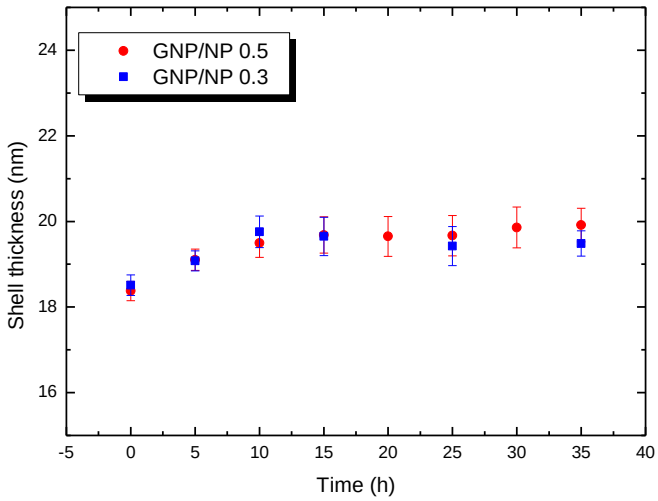

Figure 7 . Evolution of shell thickness for chitosan-TPP nanoparticles during crosslinking with genipin in water at 37°C.

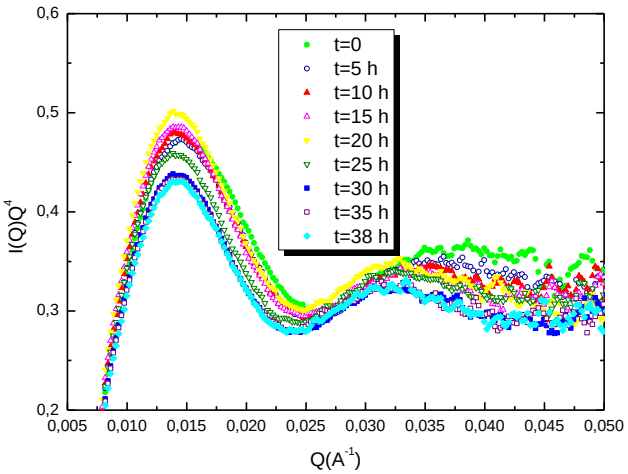

Figure 8. Porod plots ($I(Q)Q^4$ vs. Q) recorded from SAXS measurements for chitosan-TPP nanoparticles during crosslinking with genipin in water at 37°C.

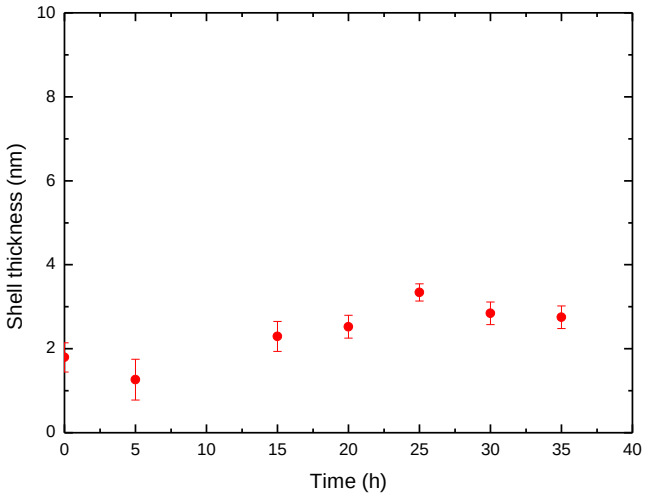

Figure 8 . Shell thickness for chitosan-TPP-ALG7006 nanoparticles during crosslinking with genipin in water at 37°C.

Experiment IV.

In Figure 9 are shown the values of shell thickness for CS-TPP nanoparticles at two distinct pHs, namely, at 1.2 (simulated gastric buffer) and at pH 4.5 (acetate buffer) and at varying degree of genipin crosslinking. Clearly, regardless of the degree of crosslinking, it was observed that the nanoparticles shell is nearly half as thinner at pH 4.5 than at 1.2. A possible explanation to account for this reduction in shell thickness is that at pH 4.5 there are proportionally less amount of protonated $-NH_3^+$ groups than at the lower pH. Hence, the lower expected electrostatic repulsion between pending chains at the nanoparticle surface can result in a more compact shell.

In turn, DLS measurements of CS-TPP nanopartices after incubation at pH 1.2 (gastric buffer) and at 4.5 (acetate buffer), revealed virtually no differences in Z-average sizes under varying concentrations of genipin (Figure 10). It was noticed that there was virtually no difference in bulk particle size after incubation at pH 1.2 or 4.5. These results are consistent with the proposal that the pH exerts mostly a local surface effect on the nanoparticles that can be probed by SAXS, but not by DLS measurements conducted on the bulk of the nanosystems. These results suggest that the sensitivity to pH, is observed only at scales (<~20 nm) well below the bulk dimensions of the nanoparticles and is somehow associated to the local effect of genipin crosslinking at the surface of the nanoparticles.

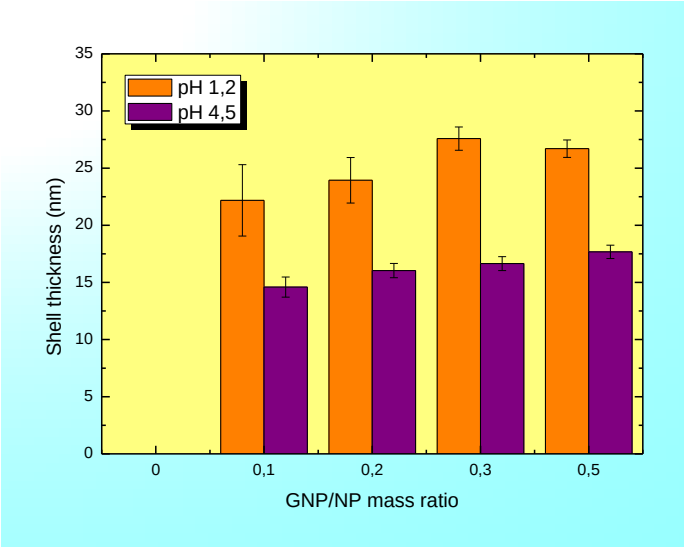

Figure 9. Shell thickness of chitosan-TPP nanoparticles at varying degrees of surface crosslinking with genipin at pH 1.2 (gastric buffer) and at 4.5 (acetate buffer) as determined by synchrotron SAXS.

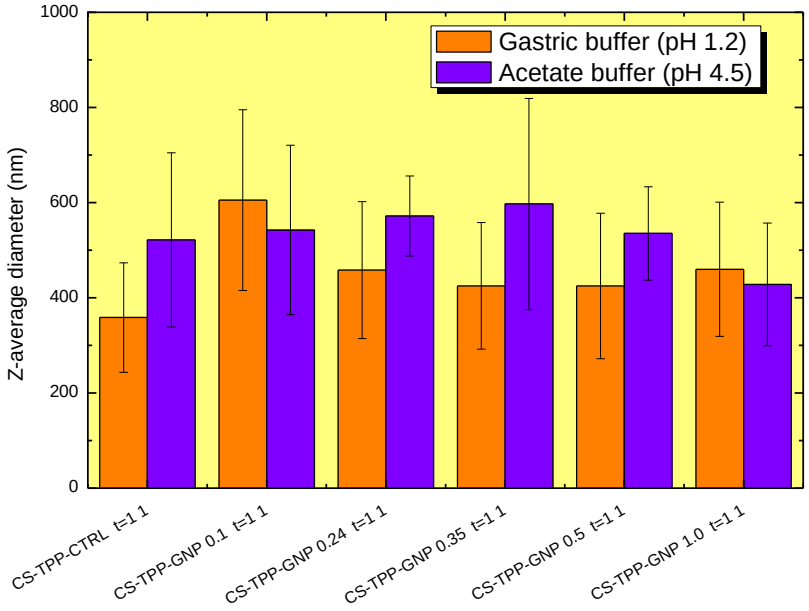

Figure 10. Z-average size measurements of chitosan-TPP nanopartices crosslinked with genipin after incubation at pH 1.2 (gastric buffer) and at 4.5 (acetate buffer) as determined by DLS.

Experiment V.

We have also investigated the role of the degree of N–acetylation (DA) of chitosan (CS) of low and high Mw (~10 and ~110 kDa denoted here as LDP CS and HDP CS, respectively), on the physicochemical properties and biological stability of oil-core nanocapsules coated with chitosan. The harnessed NCs had a rather constant average particle size (~150-200 nm) and spherical morphology, irrespective of CS's DA and Mw. The surface charge zeta potential (ζ) was invariably highly positive and exhibited a monotonic decreasing trend as the CS's DA increased and greater ζ values were recorded for HDP CS–coated NCs than for LDP CS-coated ones. We hypothesize that LDP CS arranges itself at the NC's surface in a flat conformation, while HDP CS does it forming loop-like ("train") assemblies. Synchrotron SAXS studies have revealed that diffraction peaks appear only in the systems coated with CS, while not in the naked nanoemulsion (Figure11). The calculated Bragg distances for a series of NCs varied in the range (~55 – ~67 Å) and increased with CS's DA irrespective of its Mw. As a preliminary interpretation we venture to suggest that CS's hydrophobic domains perturb the phospholipid membrane by the penetration of of CS into the oily phase, thus effectively increasing the distance between polar lecithin heads.

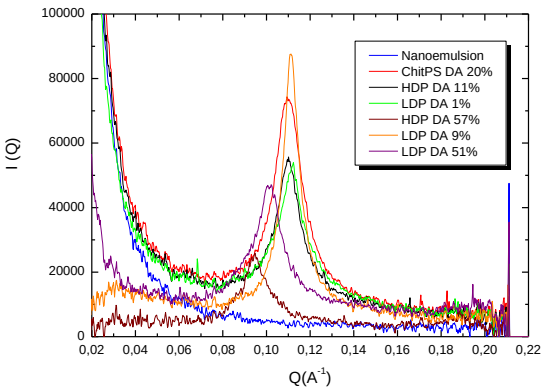

Figure 11. SAXS scattering curve for CS-coated nanocapsules and naked nanoemulsión in water at 25°C

Conclusions

- ✖ The obtained particles exhibit a core-shell structure, as probed by TEM. The thickness of the shell was found to be dependent on pH as probed by synchrotron SAXS studies.
- ✖ The obtained nanoparticles were found to be stable in a wide range of fluids of physiological relevance over a wide range of pH 1.2 o 7.4 (simulated gastric and intestinal fluids, acetate buffer and PBS).
- ✖ In oil-core nanocapsules Bragg diffractions, corresponding wityh correlation distances in the range ~55 – ~67 Å appear to be influenced by the degree of acetylation of chitosan, irrespective of its molecular weight. This could be the consequence of the phospholipid layer by chitosan, via hydrophobic association.

References

1. Couvreaur P. & Vauthier C. (2006). Pharm Res 23(7), 1417-1450.
2. Kayser O et al. (2005) Curr Pharm Biotechnol, 6, 3 - 5.
3. Bromberg L.E. & Ron E.S. (1998). Adv. Drug Deliver Rev., 31,197-221
4. Lemarchand C. et al. (2006) Biomaterials, 27,108-118
5. Roe, R. J. (2000). Methods of X-ray and neutron scattering in polymer science. New York, Oxford University Press
6. Porte, G. (2002). Surfactant Micelles and Bilayers:Shapes and Interactions. Neutrons, X-rays and Light: Scattering Methods applied to Soft Condensed Matter. P. Linder and T. Zemb. Amsterdam, Elseveier Science B.V.
7. Goycoolea F.M., Lollo G., Remuñán-López C., Quaglia F., Alonso M.J. Chitosan–alginate blended nanoparticles as carriers for transmucosal delivery of macromolecules. Biomacromolecules. 10, 1743-1743